PNAS

Supporting Information for

Dopaminergic mechanisms supporting hippocampal post-encoding dynamics in humans

Claire J. Ciampa[1]*, Thomas M. Morin[1,2], Jourdan H. Parent[1], Alex Adornato[1], Jordyn L. Cowan[1], Katherine O'Malley[1], Rachel E. Marcus[1], Charlee Gordon[1], James D. Howard[1], Arielle Tambini[3], Cristina Cusin[4], Jacob Hooker[2], Anne S. Berry[1,5]

1. Psychology Department, Brandeis University, Waltham, MA 02153
2. Martinos Center for Biomedical Imaging, Massachusetts General Hospital, Boston, MA 02129
3. Nathan Kline Institute for Psychiatric Research, Orangeburg, NY 10962
4. Depression Clinical and Research Program, Massachusetts General Hospital, Boston, MA 02114
5. Volen Center for Complex Systems, Brandeis University, Waltham, MA 02153

*Corresponding author: Claire J. Ciampa
Email: claireciampa@brandeis.edu

This PDF file includes:

Supporting Information Text

Detailed Methods

Participant Attrition and Exclusion

Our sample included 46 healthy older adults (60-82 years old, mean age = 69.24 years, SD = 5.06 years; 52% female) that underwent fMRI scanning and participated in a behavioral task. Of these 46 participants, 11 participants underwent placebo scanning only and did not have scanning data on drug. An additional 2 participants completed the task outside of the scanner due to scanner issues and 2 participants exited the scanner early, resulting in a lack of full fMRI datasets for these participants. Two participants' placebo resting state scans and 4 participants' drug resting state scans were excluded due to high levels of motion (> 20% of frames motion scrubbed). An additional 3 participants with high motion in their placebo encoding task scans and 2 participants with high motion in their drug encoding task scans were excluded from reinstatement analyses. This resulted in a final fMRI dataset of n = 40 participants with placebo resting state fMRI and n = 31 participants with drug resting state fMRI. Reinstatement analyses, which relied on both resting state and encoding task fMRI scans, included n = 37 participants on placebo and n = 29 participants on drug. Thirty-three participants had baseline (placebo) [^{11}C]raclopride PET scans. Two participants failed reconstruction due to image quality issues, resulting in a sample of n = 31 participants with placebo [^{11}C]raclopride. More details on participant attrition and exclusion are presented in **Figure S3**.

fMRI Preprocessing with fMRIPrep

The following boilerplate text was produced by the fMRIPrep pipeline that was used to preprocess the MRI data in this study:

Results included in this manuscript come from preprocessing performed using fMRIPrep (22.0.2) which is based on Nipype (1.8.5).

Preprocessing of B0 Inhomogeneity Mappings: A *B0* nonuniformity map (or *fieldmap*) was estimated from the phase-drift map(s) measure with two consecutive GRE (gradient-recalled echo) acquisitions. The corresponding phase-map(s) were phase-unwrapped with `prelude` (FSL 6.0.5.1:57b01774).

Anatomical Data Preprocessing: The T1-weighted (T1w) image was corrected for intensity non-uniformity (INU) with `N4BiasFieldCorrection` [@n4], distributed with ANTs 2.3.3 [@ants, RRID:SCR_004757], and used as T1w-reference throughout the workflow. The T1w-reference was then skull-stripped with a *Nipype* implementation of the `antsBrainExtraction.sh` workflow (from ANTs), using OASIS30ANTs as target template. Brain tissue segmentation of cerebrospinal fluid (CSF), white-matter (WM) and gray-matter (GM) was performed on the brain-extracted T1w using `fast` [FSL 6.0.5.1:57b01774, RRID:SCR_002823, @fsl_fast]. Brain surfaces were reconstructed using `recon-all` [FreeSurfer 7.2.0, RRID:SCR_001847, @fs_reconall], and the brain mask estimated previously was refined with a custom variation of the method to reconcile ANTs-derived and FreeSurfer-derived segmentations of the cortical gray-matter of Mindboggle [RRID:SCR_002438, @mindboggle]. Volume-based spatial normalization to two standard spaces (MNI152NLin2009cAsym, MNI152NLin6Asym) was performed through nonlinear registration with `antsRegistration` (ANTs 2.3.3), using brain-extracted versions of both T1w reference and the T1w template. The following templates were selected for spatial normalization: *ICBM 152 Nonlinear Asymmetrical template version 2009c* [@mni152nlin2009casym, RRID:SCR_008796; TemplateFlow ID: MNI152NLin2009cAsym], *FSL's MNI ICBM 152 non-linear 6th Generation Asymmetric Average Brain Stereotaxic Registration Model* [@mni152nlin6asym, RRID:SCR_002823; TemplateFlow ID: MNI152NLin6Asym].

Functional Data Preprocessing: For each of the four BOLD runs per subject (pre-task rest, two encoding runs, and post-task rest), the following preprocessing was performed. First, a reference volume and its skull-stripped version were generated using a custom methodology of *fMRIPrep*. Head-motion parameters with respect to the BOLD reference (transformation matrices, and six corresponding rotation and translation parameters) are estimated before any spatiotemporal filtering using `mcflirt` [FSL 6.0.5.1:57b01774, @mcflirt]. The estimated *fieldmap* was then aligned with rigid-registration to the target EPI (echo-planar imaging) reference run. The field coefficients were mapped on to the reference EPI using the transform. BOLD runs were

slice-time corrected to 1.46s (0.5 of slice acquisition range 0s-2.93s) using `3dTshift` from AFNI [@afni, RRID:SCR_005927]. The BOLD reference was then co-registered to the T1w reference using `bbregister` (FreeSurfer) which implements boundary-based registration [@bbr]. Co-registration was configured with six degrees of freedom. Several confounding time-series were calculated based on the *preprocessed BOLD*: framewise displacement (FD), DVARS and three region-wise global signals. FD was computed using two formulations following Power (absolute sum of relative motions, @power_fd_dvars) and Jenkinson (relative root mean square displacement between affines, @mcflirt). FD and DVARS are calculated for each functional run, both using their implementations in *Nipype* [following the definitions by @power_fd_dvars]. The three global signals are extracted within the CSF, the WM, and the whole-brain masks. Additionally, a set of physiological regressors were extracted to allow for component-based noise correction [*CompCor*, @compcor]. Principal components are estimated after high-pass filtering the *preprocessed BOLD* time-series (using a discrete cosine filter with 128s cut-off) for the two *CompCor* variants: temporal (tCompCor) and anatomical (aCompCor). tCompCor components are then calculated from the top 2% variable voxels within the brain mask. For aCompCor, three probabilistic masks (CSF, WM and combined CSF+WM) are generated in anatomical space. The implementation differs from that of Behzadi et al. in that instead of eroding the masks by 2 pixels on BOLD space, a mask of pixels that likely contain a volume fraction of GM is subtracted from the aCompCor masks. This mask is obtained by dilating a GM mask extracted from the FreeSurfer's *aseg* segmentation, and it ensures components are not extracted from voxels containing a minimal fraction of GM. Finally, these masks are resampled into BOLD space and binarized by thresholding at 0.99 (as in the original implementation). Components are also calculated separately within the WM and CSF masks. For each CompCor decomposition, the *k* components with the largest singular values are retained, such that the retained components' time series are sufficient to explain 50 percent of variance across the nuisance mask (CSF, WM, combined, or temporal). The remaining components are dropped from consideration. The head-motion estimates calculated in the correction step were also placed within the corresponding confounds file. The confound time series derived from head motion estimates and global signals were expanded with the inclusion of temporal derivatives and quadratic terms for each [@confounds_satterthwaite_2013]. Frames that exceeded a threshold of 0.5 mm FD or 1.5 standardized DVARS were annotated as motion outliers. Additional nuisance timeseries are calculated by means of principal components analysis of the signal found within a thin band (*crown*) of voxels around the edge of the brain, as proposed by [@patriat_improved_2017]. The BOLD time-series were resampled into several standard spaces, correspondingly generating the following *spatially-normalized, preprocessed BOLD runs*: MNI152NLin2009cAsym, MNI152NLin6Asym. First, a reference volume and its skull-stripped version were generated using a custom methodology of *fMRIPrep*. The BOLD time-series were resampled onto the following surfaces (FreeSurfer reconstruction nomenclature): *fsaverage*. All resamplings can be performed with *a single interpolation step* by composing all the pertinent transformations (i.e. head-motion transform matrices, susceptibility distortion correction when available, and co-registrations to anatomical and output spaces). Gridded (volumetric) resamplings were performed using `antsApplyTransforms` (ANTs) configured with Lanczos interpolation to minimize the smoothing effects of other kernels [@lanczos]. Non-gridded (surface) resamplings were performed using `mri_vol2surf` (FreeSurfer).

Many internal operations of *fMRIPrep* use *Nilearn* 0.9.1 [@nilearn, RRID:SCR_001362], mostly within the functional processing workflow. For more details of the pipeline, see [the section corresponding to workflows in *fMRIPrep*'s documentation] (https://fmriprep.readthedocs.io/en/latest/workflows.html "FMRIPrep's documentation").

Supplemental Results

Effects of drug and reward on context memory

We tested for effects of drug and reward on context memory (hit rate-false alarm rate) using a Drug*Reward linear mixed effects (LME) model (**Figure S1**). There was a significant main effect of Reward ($t = 2.79$, $p = .006$, $f^2 = 0.05$) such that participants demonstrated better memory for correctly matching items and background contexts when the items were viewed on the high reward background relative to the low reward background. There was no significant interaction

between reward and drug predicting context memory ($t = 1.00$, $p = .32$, $f^2 = 0.006$) and no main effect of Drug ($t = 0.82$, $p = .41$, $f^2 = 0.004$).

No relationships between reinstatement/RSFC and memory

We tested the relationship between memory and hippocampal reinstatement (post-pre pattern similarity) using a Drug*Reward*Reinstatement interaction LME model predicting item memory (**Figure S2A**). As reported under behavioral results, there were main effects of Reward ($t = 3.52$, $p = .0007$, $f^2 = 0.15$) and Drug ($t = 2.80$, $p = .006$, $f^2 = 0.08$) but no other main effects or interactions ($p > .06$), indicating that hippocampal reinstatement does not relate to item memory performance in our sample of older adults.

To investigate whether RSFC (post-pre) related to memory performance, we tested a Drug*Reward*RSFC (post-pre) interaction LME model on item memory (**Figure S2B**). Similar to the reinstatement analysis, there were significant main effects of Reward ($t = 3.35$, $p = .001$, $f^2 = 0.13$) and Drug ($t = 2.08$, $p = .04$, $f^2 = 0.04$) but no other significant main effects or interactions ($p > .07$).

*Two-way Drug*D2DR interactions*

We conducted two-way Drug*D2DR interactions (collapsing across reward) predicting pattern similarity and memory to confirm that our main findings do not change when simplifying the model. A two-way Drug*D2DR model predicting pattern similarity yielded a significant Drug*D2DR interaction ($t = 3.36$, $p = .002$, $f^2 = 0.30$). Follow-up simple linear regressions probing this interaction demonstrated that higher D2DR related to stronger pattern similarity (post-pre) on drug ($t = 3.73$, $p = .003$, $f^2 = 1.49$) but not placebo ($t = 1.02$, $p = .32$, $f^2 = 0.003$), which is consistent with the results of the three-way Drug*D2DR*Reward interaction analysis. Similarly, a two-way Drug*D2DR model predicting memory resulted in no interaction or main effects ($p > .15$), which is in line with the findings from the three-way Drug*D2DR*Reward analysis.

Figures
Fig S1

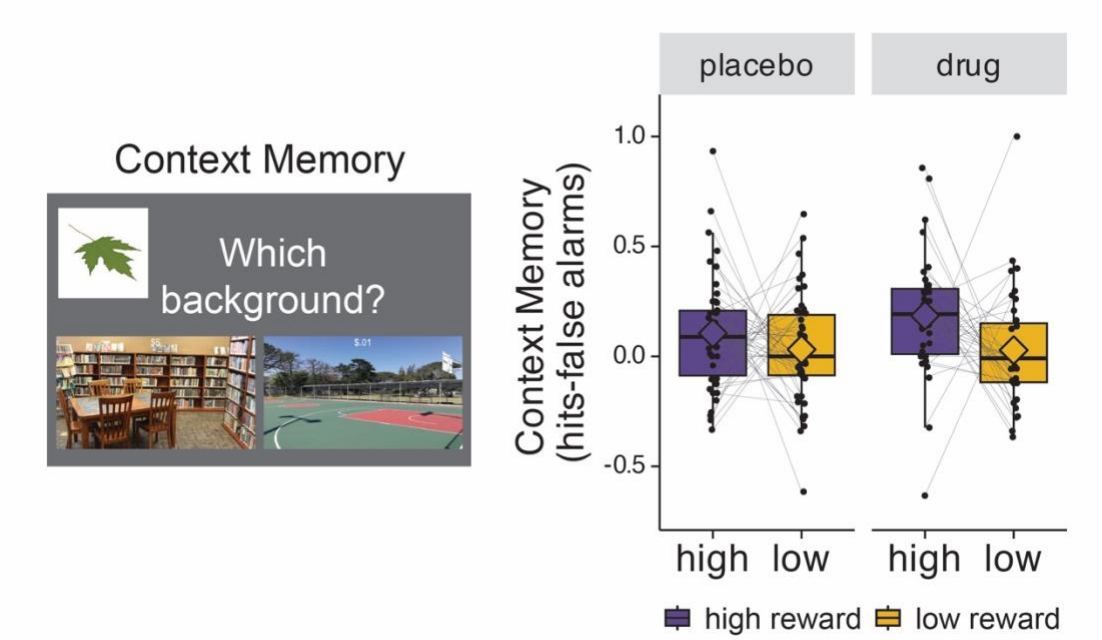

Figure S1. *Effects of drug and reward on context memory.* Context memory was assessed by asking participants to match an item with the background on which the item was viewed (high or low reward backgrounds). Boxplot shows context memory performance (hit rate-false alarm rate) split by placebo and drug for high reward (purple) and low reward (gold). Placebo n = 46, drug n = 35.

Fig S2

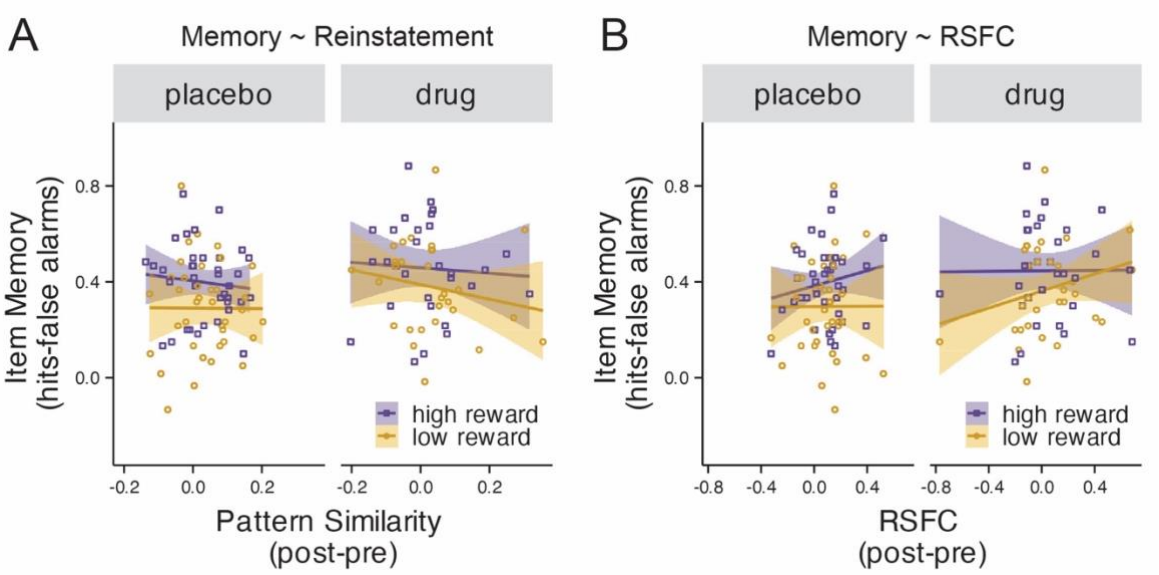

Figure S2. *Relationships between memory and fMRI measures.* (A) Scatterplot showing the relationship between item memory (hit rate-false alarm rate) and reinstatement (encoding ~ rest pattern similarity, post-pre). Panels split figure by placebo and drug. High reward is displayed in purple and low reward is displayed in gold. Placebo n = 37, drug n = 29. (B) Scatterplot showing the relationship between item memory and resting state functional connectivity (RSFC, post-pre). Placebo n = 40, drug n = 31.

Fig S3

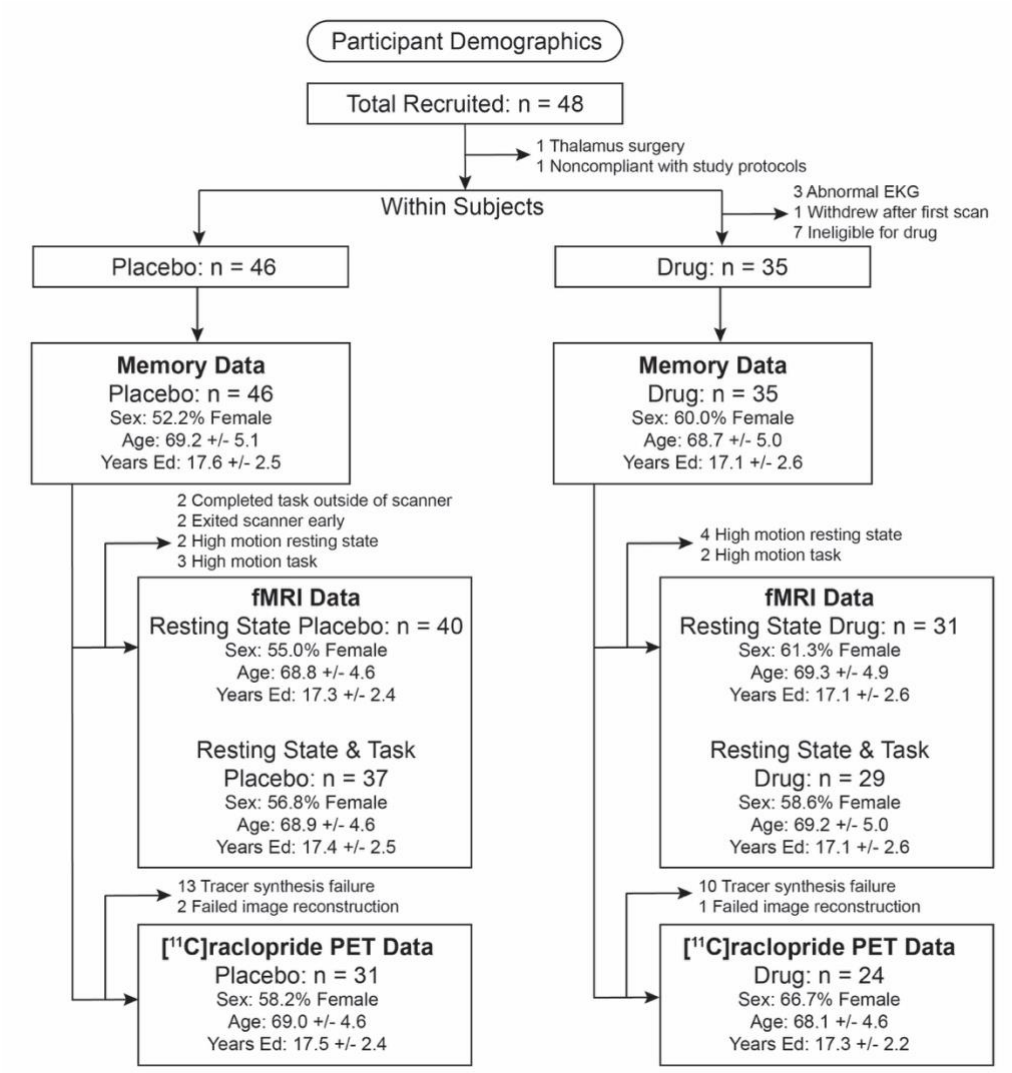

Figure S3. *Participant attrition and exclusion.* 48 cognitively normal healthy older adults were recruited. 46 participants were included in analyses. A quality control procedure was used to include/exclude participants. For participants with memory data, their available fMRI and PET imaging data was assessed for quality based on motion, PET tracer issues, and image reconstruction quality. Participants were included/excluded as noted. We attempted to include as much data as possible (e.g., if a participant had fMRI data but not PET data, we included their fMRI data in fMRI analyses, but not in analyses that included both fMRI and PET).

Table S1.
*Drug*Reward interaction on item memory using a linear mixed effects (LME) model. The dependent variable is adjusted hit rate (hit rate - false alarm rate). Covariates include age, sex, years of education, and weight.*

Variable	Unstandardized Coef.	SE	t-value	p-value	95% CI (Lower)	95% CI (Upper)
Item Memory ~ Drug*Reward + Age + Sex + YearsEd + Weight						
(Intercept)	0.12	0.38	0.32	.75	-0.64	0.88
Drug	0.03	0.01	2.87	<.01	0.01	0.06
Reward	0.04	0.01	3.98	<.01	0.02	0.06
Age	0.00	0.00	0.43	.67	-0.01	0.01
Sex	0.07	0.05	1.36	.18	-0.04	0.18
Years Ed	-0.00	0.01	-0.54	.59	-0.02	0.01
Weight	0.00	0.00	1.01	.32	-0.00	0.00
Drug*Reward	-0.00	0.01	-0.46	.64	-0.03	0.02

Table S2.
*(A) Drug*Reward*Stage interaction linear mixed effects (LME) model on pattern similarity. (B) Drug*Stage interaction LME model on resting state functional connectivity (RSFC). Models adjust for age, sex, years of education, and weight as covariates.*

Variable	Unstandardized Coef.	SE	t-value	p-value	95% CI (Lower)	95% CI (Upper)
(A) Pattern similarity ~ Drug*Reward*Stage + Age + Sex + YearsEd + Weight						
(Intercept)	0.31	0.19	1.61	.12	-0.08	0.70
Drug	-0.00	0.00	-0.12	.90	-0.01	0.01
Reward	0.00	0.00	0.01	.99	-0.01	0.01
Stage	0.01	0.00	3.23	<.01	0.01	0.02
Age	0.00	0.00	2.53	.02	0.00	0.01
Sex	-0.06	0.03	-2.23	.03	-0.12	-0.00
Years Ed	0.00	0.00	0.78	.44	-0.01	0.01
Weight	-0.00	0.00	-1.18	.25	-0.00	0.00
Drug*Reward	-0.00	0.00	-1.19	.23	-0.01	0.00
Drug*Stage	-0.00	0.00	-0.46	.65	-0.01	0.01
Reward*Stage	-0.00	0.00	-0.45	.65	-0.01	0.01
Drug*Reward*Stage	-0.00	0.00	-0.48	.63	-0.01	0.01
(B) Resting State Functional Connectivity (RSFC) ~ Drug*Stage + Age + Sex + YearsEd + Weight						
(Intercept)	1.42	0.37	3.82	<.01	0.67	2.18
Drug	0.02	0.01	1.41	.16	-0.01	0.04
Stage	0.03	0.01	2.48	.01	0.01	0.06
Age	-0.01	0.00	-2.60	.01	-0.02	-0.00
Sex	-0.07	0.05	-1.26	.22	-0.17	0.04
Years Ed	0.01	0.01	0.67	.51	-0.01	0.03
Weight	-0.00	0.00	-1.89	.07	-0.00	0.00
Drug*Stage	-0.01	0.01	-0.80	.43	-0.04	0.01

Table S3

(A) Relationship between baseline dorsal caudate D2DR and reinstatement (pattern similarity, post-pre). (B) Relationship between baseline dorsal caudate D2DR and resting state functional connectivity. (C) Relationship between baseline dorsal caudate D2DR and item memory (hit rate-false alarm rate). Models are linear mixed effects (LME) models adjusting for age, sex, years of education, and weight.

Variable	Unstandardized Coef.	SE	t-value	p-value	95% CI (Lower)	95% CI (Upper)
A. Pattern Similarity (post-pre) ~ D2DR*Drug*Reward + Age + Sex + YearsEd + Weight						
(Intercept)	-1.05	0.34	-3.13	.01	-1.75	-0.34
D2DR	0.23	0.06	3.85	<.01	0.10	0.35
Drug	-0.35	0.08	-4.66	<.01	-0.50	-0.20
Reward	0.03	0.07	0.49	.63	-0.11	0.18
Age	0.00	0.00	1.47	.16	-0.00	0.01
Sex	0.06	0.04	1.54	.14	-0.02	0.14
Years Ed	0.01	0.00	1.36	.19	-0.00	0.02
Weight	0.00	0.00	0.91	.38	-0.00	0.00
D2DR*Drug	0.16	0.03	4.74	<.01	0.09	0.23
D2DR*Reward	-0.02	0.03	-0.57	.57	-0.08	0.05
Drug*Reward	0.02	0.07	0.24	.81	-0.12	0.16
D2DR*Drug*Reward	-0.01	0.03	-0.32	.75	-0.07	0.05
B. RSFC (post-pre) ~ D2DR*Drug + Age + Sex + YearsEd + Weight						
(Intercept)	-0.02	0.80	-0.02	.98	-1.66	1.62
D2DR	0.25	0.14	1.78	.09	-0.04	0.53
Drug	-0.74	0.23	-3.21	<.01	-1.21	-0.26
Age	-0.00	0.01	-0.11	.92	-0.01	0.01
Sex	-0.04	0.09	-0.50	.62	-0.22	0.14
Years Ed	-0.01	0.01	-0.48	.64	-0.03	0.02
Weight	-0.00	0.00	-1.31	.20	-0.00	0.00
D2DR*Drug	0.34	0.10	3.33	<.01	0.13	0.56

Item Memory ~ D2DR*Drug*Reward + Age + Sex + YearsEd + Weight						
(Intercept)	0.56	0.80	0.70	.49	-1.08	2.20
D2DR	-0.17	0.14	-1.25	.22	-0.45	0.11
Drug	-0.06	0.11	-0.56	.58	-0.27	0.15
Reward	0.28	0.10	2.83	.01	0.08	0.48
Age	0.00	0.01	0.10	.92	-0.01	0.01
Sex	0.05	0.08	0.55	.59	-0.13	0.22
Years Ed	-0.00	0.01	-0.07	.94	-0.03	0.03
Weight	0.00	0.00	0.77	.45	-0.00	0.00
D2DR*Drug	0.05	0.05	0.97	.33	-0.05	0.14
D2DR*Reward	-0.11	0.04	-2.48	.02	-0.20	-0.02
Drug*Reward	-0.08	0.10	-0.86	.39	-0.28	0.11
D2DR*Drug*Reward	0.03	0.04	0.76	.45	-0.06	0.12
D2DR*Drug*Reward	0.03	0.04	0.83	.41	-0.05	0.12